VNU Journal of Science: Mathematics – Physics, Vol. 32, No. 1 (2016) 1-19

Vibration and Nonlinear Dynamic Analysis of Imperfect Thin Eccentrically Stiffened Functionally Graded Plates in Thermal Environments

Pham Hong Cong, Nguyen Dinh Duc*

University of Engineering and Technology, Vietnam National University, Hanoi, 144 Xuan Thuy, Cau Giay, Hanoi, Vietnam

Received 20 August 2015
Revised 27 February 2016; Accepted 14 March 2016

Abstract: This paper presents an analytical approach to investigate the vibration and nonlinear dynamic response of imperfect thin eccentrically stiffened functionally graded material (FGM) plates in thermal environments using the classical plate theory, stress function and the Lekhnitsky smeared stiffeners technique. Material properties are assumed to be temperature-dependent, and two types of thermal condition are investigated: the uniform temperature rise; and the temperature gradient through the thickness. Numerical results for vibration and nonlinear dynamic response of the imperfect eccentrically stiffened FGM plates are obtained by the Runge-Kutta method. The results show the influences of geometrical parameters, material properties, imperfections, eccentric stiffeners, and temperature on the vibration and nonlinear dynamic response of FGM plates. The numerical results in this paper are compared with the results reported in other publications.

Keywords: Vibration, nonlinear dynamic response, thin eccentrically stiffened FGM plates, classical plate theory, thermal environments.

1. Introduction

Functionally graded materials (FGMs) are homogeneous composite and microscopic-scale materials with the mechanical and thermal properties varying smoothly and continuously from one surface to the other. Typically, these materials are made from a mixture of metal and ceramic, or a combination of different metals by gradually varying the volume fraction of the constituent metals. The properties of FGM plates are assumed to vary through the thickness of the structure. Due to their high heat resistance, FGMs have many practical applications, such as use in reactor vessels, aircrafts, space vehicles, defense industries, and other engineering structures.

Therefore, many investigations have been carried out on the dynamic and vibration response of FGM plates. Woo et al. [1] investigated the nonlinear free vibration behavior of functionally graded plates; and Wu et al. [2] published their results on the nonlinear static and dynamic analysis of

* Tel.: 84-915966626
Email: ducnd@vnu.edu.vn

functionally graded plates. Matsunaga [3] studied the free vibration and stability of FGM plates according to a 2D high order deformation theory. Allahverdizadeh et al. [4] studied the nonlinear free and forced vibration analysis of circular functionally graded plates. Alijani et al. [5] and Chorfi and Houmat [6] studied the nonlinear vibration response of functionally graded doubly-curved shallow shells. Kim [7] studied the geometrically nonlinear analysis of functionally graded material (FGM) plates and shells using a four-node quasi-conforming shell element. Mollarazi et al. [8] studied analysis of free vibration of functionally graded material (FGM) cylinders by a meshless method. Jahanghiry et al. [9] have applied the stability analysis of FGM microgripper subjected to nonlinear electrostatic and temperature variation loadings. Kamran Asemi et al. [10] have investigated the three-dimensional natural frequency analysis of anisotropic functionally graded annular sector plates resting on elastic foundations.

To date, the dynamic analysis of FGM plates with temperature-dependent material properties has received much attention from researchers. Huang and Shen [11] studied the vibration and dynamic response of FGM plates in thermal environments and the material properties are assumed to be temperature-dependent. Kim [12] studied the temperature-dependent vibration analysis of functionally graded rectangular plates by the finite element method, and the Rayleigh-Ritz procedure was applied to obtain the frequency equation. Fakhari and Ohadi [13] studied the nonlinear vibration control of functionally graded plates with piezoelectric layers in thermal environments using the finite element method. In their study, the material properties of FGMs have also been assumed to be temperature-dependent and graded in the thickness direction according to a simple power law distribution in terms of the volume fractions of the constituents. We should mention that all the above results have been investigated under higher order shear deformation theory using the displacement functions.

FGM plates, like other composite structures, are usually reinforced by stiffening members to provide the benefit of added load-carrying static and dynamic capability with a relatively small additional weight penalty. Investigation of the static and dynamic capability of eccentrically stiffened FGM structures has received comparatively little attention. Bich et al. studied the nonlinear post-buckling and dynamic response of eccentrically stiffened functionally graded plates [14] and panels [15]. Duc [16] investigated the nonlinear dynamic response of imperfect eccentrically stiffened doubly-curved FGM shallow shells on elastic foundations. It is noted that in all the publications mentioned above [14, 15, 16], the eccentrically stiffened FGM plates and shells are considered without temperature. Duc et al. [17, 18] investigated the nonlinear static post-buckling of imperfect eccentrically stiffened FGM doubly-curved shallow shells and plates resting on elastic foundations in thermal environments. Bich et al. [19] investigated the nonlinear vibration of imperfect eccentrically stiffened FGM doubly-curved shallow shells using the first order shear deformation theory. Quan et al. [20] investigated the nonlinear dynamic analysis and vibration of shear deformable eccentrically stiffened S-FGM cylindrical panels. Duc and Cong [21] studied the nonlinear dynamic response of imperfect FGM plates, and Duc and Quan [22] studied doubly-curved shallow shells. In the two studies, stiffeners had not been used, and the study by Duc and Cong [21] did not mention temperature-dependence. Recently, Duc et al., [23] studied the nonlinear stability of shear deformable eccentrically stiffened functionally graded plates on elastic foundations with temperature-dependent properties. There are no publications on the vibration and nonlinear dynamic response of FGM plates reinforced with eccentric stiffeners under temperature. The most difficult part in this type of problem is to calculate the thermal mechanism of FGM plates as well as eccentric stiffeners under thermal loads.

This paper presents an analytical approach to investigate the vibration and nonlinear dynamic response of imperfect eccentrically stiffened FGM plates with temperature-dependent material properties in thermal environments using classical plate theory, the Lekhnitsky smeared stiffeners

technique and Bubnov-Galerkin method. The study also analysed the effect of temperature, imperfection, geometrical parameters, and volume fraction on the vibration and nonlinear dynamic response of imperfect eccentrically stiffened FGM plates.

2. Rectangular eccentrically stiffened FGM plate (ES-FGM)

Consider a rectangular ES-FGM plate of length a, width b and thickness h. A coordinate system (x, y, z) is chosen so that the (x, y) plane is on the middle surface of the plate and the z-axis is the thickness direction

$(-h/2 \le z \le h/2)$, as shown in Fig 1.

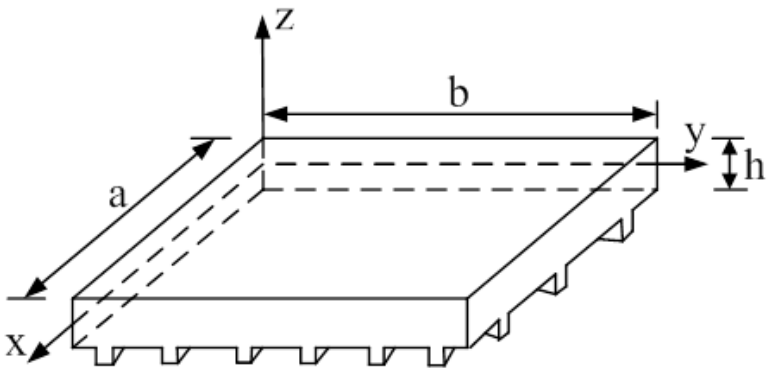

Fig. 1. Geometry and coordinate system of an eccentrically stiffened FGM plate.

The effective properties, modulus of elasticity E, mass density ρ, coefficient of thermal expansion α, and the coefficient of thermal conduction K of the FGM plate can be written as follows [17, 18, 24]:

$$\begin{aligned}&\left[E(z,T),\rho(z,T),\alpha(z,T),K(z,T)\right]=\left[E_m(T),\rho_m(T),\alpha_m(T),K_m(T)\right]\\&+\left[E_{cm}(T),\rho_{cm}(T),\alpha_{cm}(T),K_{cm}(T)\right]\left(\frac{2z+h}{2h}\right)^k\end{aligned} \tag{1}$$

in which the Poisson's ratio is assumed constant ($\nu = const$),

$$E_{cm}(T)=E_c(T)-E_m(T),\ \rho_{cm}(T)=\rho_c(T)-\rho_m(T),$$
$$\alpha_{cm}(T)=\alpha_c(T)-\alpha_m(T),\ K_{cm}(T)=K_c(T)-K_m(T)$$

and h is the thickness of the plate; $0 \le k \le \infty$ is the volume fraction index; and m and c denote metal and ceramic constituents, respectively.

Young's modulus of elasticity E, thermal expansion coefficient α, coefficient of heat transfer K, and mass density ρ can be expressed as a function of temperature, as [24]:

$$\mathrm{Pr} = P_0\left(P_{-1}T^{-1}+1+P_1T^1+P_2T^2+P_3T^3\right) \tag{2}$$

where $T = T_0 + \Delta T(z)$, T_0 is room temperature; and $P_0, P_{-1}, P_1, P_2, P_3$ are coefficients and dependent only on the constitutent material. For brevity, this paper will denote T-D for the temperature-dependent case, and T-ID for the temperature-independent case.

3. Governing equations

Using classical plate theory for thin plates and geometrical nonlinear cases, the strains at the middle surface and curvatures are related to the displacement components u, v, w in the x, y, z coordinate directions as [24]:

$$\begin{pmatrix} \varepsilon_x^0 \\ \varepsilon_y^0 \\ \gamma_{xy}^0 \end{pmatrix} = \begin{pmatrix} \dfrac{\partial u}{\partial x} + \dfrac{1}{2}\left(\dfrac{\partial w}{\partial x}\right)^2 \\ \dfrac{\partial v}{\partial y} + \dfrac{1}{2}\left(\dfrac{\partial w}{\partial y}\right)^2 \\ \dfrac{\partial u}{\partial y} + \dfrac{\partial v}{\partial x} + \dfrac{\partial w}{\partial x}\dfrac{\partial w}{\partial y} \end{pmatrix}, \begin{pmatrix} k_x \\ k_y \\ k_{xy} \end{pmatrix} = \begin{pmatrix} -w_{,xx} \\ -w_{,yy} \\ -w_{,xy} \end{pmatrix} \tag{3}$$

The strains across the plate thickness at a distance z from the mid-surface are:

$$\begin{pmatrix} \varepsilon_x \\ \varepsilon_y \\ \gamma_{xy} \end{pmatrix} = \begin{pmatrix} \varepsilon_x^0 \\ \varepsilon_y^0 \\ \gamma_{xy}^0 \end{pmatrix} + z \begin{pmatrix} k_x \\ k_y \\ 2k_{xy} \end{pmatrix} \tag{4}$$

The strains from Eq. (3) must be relative in the deformation compatibility equation:

$$\frac{\partial^2 \varepsilon_x^0}{\partial y^2} + \frac{\partial^2 \varepsilon_y^0}{\partial x^2} - \frac{\partial^2 \gamma_{xy}^0}{\partial x \partial y} = \frac{\partial^2 w}{\partial x \partial y} - \frac{\partial^2 w}{\partial x^2}\frac{\partial^2 w}{\partial y^2} \tag{5}$$

Hooke's law for a plate, including the thermal effects, is:

$$\left(\sigma_x^p, \sigma_y^p\right) = \frac{E(z,T)}{1-\nu^2}[(\varepsilon_x, \varepsilon_y) + \nu\left(\varepsilon_y, \varepsilon_x\right) - (1+\nu)\alpha(z,T)\Delta T(z)(1,1)] \tag{6}$$

$$\sigma_{xy}^p = \frac{E(z,T)}{2(1+\nu)}\gamma_{xy}$$

and for the stiffeners [24] is:

$$(\sigma_x^{st}, \sigma_y^{st}) = E_0(\varepsilon_x, \varepsilon_y) - \frac{E_0}{1-2\nu_0}\alpha_0(T)\Delta T(1,1) \tag{7}$$

Where ΔT is the temperature rise in the plate, and $\Delta T = \Delta T(z)$ in the general case. $E(z,T)$ and $\alpha(z,T)$ are defined by Eq. (2). $E_0(T)$ and $\alpha_0(T)$ are Young's modulus and the thermal expansion coefficient of stiffeners. The FGM plate reinforced by eccentric longitudinal and transverse stiffeners is shown in Fig.1. E_0 is the elasticity modulus in the axial direction of the corresponding stiffener, which is assumed to be identical for both types of longitudinal and transverse stiffeners. In order to provide continuity between the plate and stiffeners, it is assumed that the stiffeners are made of full

metal $(E_0 = E_m)$ if putting them at the metal-rich side of the plate, and conversely, full ceramic stiffeners $(E_0 = E_c)$ at the ceramic-rich side of the plate.

The contribution of stiffeners can be accounted for using the Lekhnitsky smeared stiffeners technique. Then integrating the stress-strain equations and their moments through the thickness of the plate, the expressions for force and moment resultants of an eccentrically stiffened FGM plate are obtained [24]:

$$\begin{aligned}
N_x &= (P_{11} + \frac{E_0^T A_1^T}{s_1^T})\varepsilon_x^0 + P_{12}\varepsilon_y^0 + (J_{11} + F_1^T)k_x + J_{12}k_y + \Phi_1 \\
N_y &= P_{12}\varepsilon_x^0 + (P_{22} + \frac{E_0^T A_2^T}{s_2^T})\varepsilon_y^0 + J_{12}k_x + (J_{22} + F_2^T)k_y + \Phi_1 \\
N_{xy} &= P_{66}\gamma_{xy}^0 + 2J_{66}k_{xy} \\
M_x &= (J_{11} + F_1^T)\varepsilon_x^0 + J_{12}\varepsilon_y^0 + (H_{11} + \frac{E_0^T I_1^T}{s_1^T})k_x + H_{12}k_y + \Phi_2 \\
M_y &= J_{12}\varepsilon_x^0 + (J_{22} + F_2^T)\varepsilon_y^0 + H_{12}k_x + (H_{22} + \frac{E_0^T I_2^T}{s_2^T})k_y + \Phi_2 \\
M_{xy} &= J_{66}\gamma_{xy}^0 + 2H_{66}k_{xy}
\end{aligned} \tag{8a}$$

where:

$$\begin{aligned}
&P_{11} = P_{22} = \frac{E_1}{1-\nu^2}, P_{12} = \frac{E_1\nu}{1-\nu^2}, P_{66} = \frac{E_1}{2(1+\nu)} \\
&J_{11} = J_{22} = \frac{E_2}{1-\nu^2}, J_{12} = \frac{E_2\nu}{1-\nu^2} J_{66} = \frac{E_2}{2(1+\nu)} \\
&H_{11} = H_{22} = \frac{E_3}{1-\nu^2}, H_{12} = \frac{E_3\nu}{1-\nu^2}, H_{66} = \frac{E_3}{2(1+\nu)} \\
&\Phi_1 = -\int_{-\frac{h}{2}}^{\frac{h}{2}} \frac{E(z)\alpha(z)\Delta T(z)}{1-\nu} dz \\
&\Phi_2 = -\int_{-\frac{h}{2}}^{\frac{h}{2}} \frac{E(z)\alpha(z)z\Delta T(z)}{1-\nu} dz
\end{aligned} \tag{8b}$$

$$E_1 = \left[\mathrm{E}_m(\mathrm{T}) + \frac{\mathrm{E}_{cm}(\mathrm{T})}{k+1} \right] \mathrm{h}, \ \mathrm{E}_2 = \frac{E_{cm}(T)kh^2}{2(k+1)(k+2)},$$

$$E_3 = \left[\frac{E_m(T)}{12} + \mathrm{E}_{cm}(\mathrm{T})\left(\frac{1}{k+3} - \frac{1}{k+2} + \frac{1}{4k+4}\right) \right] \mathrm{h}^3,$$

$$I_1^T = \frac{d_1^T (h_1^T)^3}{12} + A_1^T (z_1^T)^2, \ I_2^T = \frac{d_2^T (h_2^T)^3}{12} + A_2^T (z_2^T)^2$$

$$F_1^T = \frac{E_0 A_1^T z_1^T}{s_1^T}, \ F_2^T = \frac{E_0 A_2^T z_2^T}{s_2^T}$$

$$z_1^T = \frac{h_1^T + h^T}{2}, \ z_2^T = \frac{h_2^T + h^T}{2}$$

in which

$$\begin{aligned}
&d_1^T = d_1(1+\alpha_m\Delta T(z)), d_2^T = d_2(1+\alpha_m\Delta T(z)),\\
&z_1^T = z_1(1+\alpha_m\Delta T(z)), z_2^T = z_2(1+\alpha_m\Delta T(z)),\\
&s_1^T = s_1(1+\alpha_m\Delta T(z)), s_2^T = s_2(1+\alpha_m\Delta T(z))
\end{aligned} \tag{9}$$

where s_1, s_2 are the spacings of the longitudinal and transverse stiffeners; I_1, I_2, z_1, z_2 are the second moments of the cross-section areas and the eccentricities of the stiffeners with respect to the middle surface of the plate, respectively; and the width and thickness of the longitudinal and transverse stiffeners are denoted by d_1, h_1 and d_2, h_2, respectively. The quantities A_1, A_2 are the cross-sectional areas of the stiffeners.

The nonlinear motion equation of the ES-FGM plate based on classical plate theory with Volmir's assumption [25] $u << w, v << w, \rho_1\frac{\partial^2 u}{\partial t^2} \to 0,\ \rho_1\frac{\partial^2 v}{\partial t^2} \to 0$ is given by:

$$\begin{aligned}
&\frac{\partial N_x}{\partial x} + \frac{N_{xy}}{\partial y} = 0\\
&\frac{\partial N_{xy}}{\partial x} + \frac{\partial N_y}{\partial y} = 0\\
&\frac{\partial^2 M_x}{\partial x^2} + 2\frac{\partial^2 M_{xy}}{\partial x\partial y} + \frac{\partial^2 M_y}{\partial y^2} + N_x\frac{\partial^2 w}{\partial x^2} + 2N_{xy}\frac{\partial^2 w}{\partial x\partial y} + N_y\frac{\partial^2 w}{\partial y^2} + q_0 = \rho_1\frac{\partial^2 w}{\partial t^2}
\end{aligned} \tag{10}$$

where:

$$\rho_1 = \left(\rho_m + \frac{\rho_c - \rho_m}{k+1}\right)h + \rho_0\left(\frac{A_1^T}{s_1^T} + \frac{A_2^T}{s_2^T}\right)$$

From Eq. (8a), reversely calculate to obtained

$$\begin{aligned}
&\varepsilon_x^0 = P_{22}^* N_x - P_{12}^* N_y + J_{11}^* w_{,xx} + J_{12}^* w_{,yy} - (P_{22}^* - P_{12}^*)\Phi_1\\
&\varepsilon_y^0 = P_{11}^* N_y - P_{12}^* N_x + J_{21}^* w_{,xx} + J_{22}^* w_{,yy} - (P_{11}^* - P_{12}^*)\Phi_1\\
&\gamma_{xy}^0 = P_{66}^* N_{xy} + 2J_{66}^* w_{,xy}
\end{aligned} \tag{11}$$

with

$$\begin{aligned}
&P_{11}^* = \frac{1}{\Delta}(P_{11} + \frac{E_0^T A_1^T}{s_1^T}),\ P_{22}^* = \frac{1}{\Delta}(P_{22} + \frac{E_0^T A_2^T}{s_2^T});\ P_{12}^* = \frac{P_{12}}{\Delta}, P_{66}^* = \frac{1}{P_{66}}\\
&\Delta = (P_{11} + \frac{E_0^T A_1^T}{s_1^T})(P_{22} + \frac{E_0^T A_2^T}{s_2^T}) - P_{12}^2\\
&J_{11}^* = P_{22}^*(J_{22} + F_1^T) - P_{12}J_{21},\\
&J_{22}^* = P_{11}^*(J_{22} + F_2^T) - P_{12}^* J_{12},\\
&J_{12}^* = P_{22}^* J_{12} - P_{12}^*(J_{22} + F_2^T),\\
&J_{21}^* = P_{11}^* J_{12} - P_{12}^*(J_{11} + F_1^T),\\
&J_{66}^* = \frac{J_{66}}{P_{66}}
\end{aligned}$$

Considering the first two equations of Eqs. (10), a stress function φ may be defined as:

$$N_x = \frac{\partial^2 \varphi}{\partial y^2}, N_y = \frac{\partial^2 \varphi}{\partial x^2}, N_{xy} = -\frac{\partial^2 \varphi}{\partial x \partial y} \tag{12}$$

Substituting Eq. (12) into Eq. (11) and substituting the result obtained into the third equation of Eqs. (10) leads to:

$$\begin{aligned} &J_{21}^* \frac{\partial^4 \varphi}{\partial x^4} + J_{12}^* \frac{\partial^4 \varphi}{\partial y^4} + (J_{11}^* + J_{22}^* - 2J_{66}^*) \frac{\partial^4 \varphi}{\partial x^2 \partial y^2} - H_{11}^* \frac{\partial^4 w}{\partial x^4} - H_{22}^* \frac{\partial^4 w}{\partial y^4} - (H_{12}^* + H_{21}^* + 4H_{66}^*) \frac{\partial^4 w}{\partial x^2 \partial y^2} \\ &+ N_x \frac{\partial^2 w}{\partial x^2} + 2N_{xy} \frac{\partial^2 w}{\partial x \partial y} + N_y \frac{\partial^2 w}{\partial y^2} + q_0 = \rho_1 \frac{\partial^2 w}{\partial t^2} \end{aligned} \tag{13}$$

where:

$$H_{11}^* = H_{11} + \frac{E_0^T I_1^T}{s_1^T} - (J_{11} + F_1^T) J_{11}^* - J_{12} J_{21}^*$$

$$H_{22}^* = H_{22} + \frac{E_0^T I_2^T}{s_2^T} - J_{12} J_{12}^* - (J_{22} + F_2^T) J_{22}^*$$

$$H_{12}^* = H_{12} - (J_{11} + F_1^T) J_{12}^* - J_{12} J_{22}^*$$

$$H_{21}^* = H_{12} - J_{12} J_{11}^* - (J_{22} + F_2^T) J_{21}^*$$

$$H_{66}^* = H_{66} - J_{66} J_{66}^*$$

For the initial imperfect ES-FGM plate, the motion equation is modified into the form:

$$\begin{aligned} &J_{21}^* \varphi_{,xxxx} + J_{12}^* \varphi_{,yyyy} + (J_{11}^* + J_{22}^* - 2J_{66}^*) \varphi_{,xxyy} - H_{11}^* w_{,xxxx} - H_{22}^* w_{,yyyy} - (H_{12}^* + H_{21}^* + 4H_{66}^*) w \\ &+ \varphi_{,yy} \left(w_{,xx} + w_{,xx}^* \right) - 2\varphi_{,xy} \left(w_{,xy} + w_{,xy}^* \right) + \varphi_{,xx} \left(w_{,yy} + w_{,yy}^* \right) + q_0 = \rho_1 \frac{\partial^2 w}{\partial t^2} \end{aligned} \tag{14}$$

where $w^*(x, y)$ denotes a known small imperfection of the initial shape of the plate. Therefore, the deformation compatibility equation of imperfect ES-FGM plates is modified to the following form:

$$\frac{\partial^2 \varepsilon_x^0}{\partial y^2} + \frac{\partial^2 \varepsilon_y^0}{\partial x^2} - \frac{\partial^2 \gamma_{xy}^0}{\partial x \partial y} = \left(\frac{\partial^2 w}{\partial x \partial y} \right)^2 - \frac{\partial^2 w}{\partial x^2} \frac{\partial^2 w}{\partial y^2} + 2 \frac{\partial^2 w}{\partial x \partial y} \frac{\partial^2 w^*}{\partial x \partial y} - \frac{\partial^2 w}{\partial x^2} \frac{\partial^2 w^*}{\partial y^2} - \frac{\partial^2 w}{\partial y^2} \frac{\partial^2 w^*}{\partial x^2} \tag{15}$$

Substituting Eqs. (11) and (12) into Eq. (15) leads to:

$$\begin{aligned} &P_{11}^* \varphi_{,xxxx} + P_{22}^* \varphi_{,yyyy} + (P_{66}^* - 2P_{12}^*) \varphi_{,xxyy} + J_{21}^* w_{,xxxx} + J_{12}^* w_{,yyyy} + (J_{11}^* + J_{22}^* - 2J_{66}^*) w_{,xxyy} \\ &- \left(w_{,xy}^2 - w_{,xx} w_{,yy} + 2w_{,xy} w_{,xy}^* - w_{,xx} w_{,yy}^* - w_{,yy} w_{,xx}^* \right) = 0 \end{aligned} \tag{16}$$

Eqs. (14) and (16) (with coefficients $J_{21}^*, J_{12}^*, J_{11}^*, ... H_{11}^*, H_{22}^*, ... P_{11}^*, P_{22}^*, ...$, which are explicit temperature-dependent) are used to investigate the nonlinear and dynamic stability of ES-FGM in thermal environments with temperature-dependent material properties. They are two nonlinear equations of two variable unknowns, w and φ.

4. Solution of the governing equations

We consider a simply supported ES-FGM imperfect plate subject to in-plane compressive loads of N_{x0} and N_{y0}, and uniformly distributed pressure of intensity q_0. In this case, the boundary conditions are:

$$\begin{aligned} &w = u = M_x = 0, N_x = N_{x0} \ \ at \ \ x = 0, a \\ &w = \mathrm{v} = M_y = 0, N_y = N_{y0} \ \ at \ \ y = 0, b \end{aligned} \tag{17}$$

The approximate solutions of Eqs. (14) and (16) satisfying the mentioned conditions in Eq. (17) are chosen in the following form:

$$\left(w, w^*\right) = \left(f(t), f_0\right) \sin \lambda_m x \sin \delta_n y \tag{18}$$

$$\varphi = A_1 \cos 2\lambda_m x + A_2 \cos 2\delta_n y + A_3 \sin \lambda_m x \sin \delta_n y + A_4 \cos \lambda_m x \cos \delta_n y + \frac{1}{2} N_{x0} y^2 + \frac{1}{2} N_{y0} x^2$$

in which $\lambda_m = m\pi / a$; $\delta_n = n\pi / b$; $f(t)$ is the total amplitude of the ES-FGM plate; m and n are the half-wave numbers along the x-axis and the y-axis, respectively; and f_0 denotes the initial imperfection of the ES-FGM plate.

Setting Eqs. (18) into Eq. (16) and solving for the unknown function φ, we obtain:

$$A_1 = \frac{\delta_n^2}{32 P_{11}^* \lambda_m^2} f(f + 2f_0); \ A_2 = \frac{\lambda_m^2}{32 P_{22}^* \delta_n^2} f(f + 2f_0)$$

$$A_3 = -\frac{J_{21}^* \lambda_m^4 + J_{12}^* \delta_n^4 + (J_{11}^* + J_{22}^* - 2J_{66}^*) \lambda_m^2 \delta_n^2}{P_{11}^* \lambda_m^4 + P_{22}^* \delta_n^4 + (P_{66}^* - 2P_{12}^*) \lambda_m^2 \delta_n^2} f;$$

$$A_4 = 0.$$

Substituting Eqs. (18) into Eq. (14) and applying the Galerkin method, we obtain the result:

$$\begin{aligned} &\frac{ab}{4} \rho_1 \ddot{f}(t) + \frac{ab}{4} \left(\frac{J^{*2}}{P^*} + H^*\right) f + \frac{2mn\pi^2 \mu_m \mu_n}{3ab} \frac{J^*}{P^*} f\left(f + f_0\right) \\ &+ \frac{1mn\pi^2}{6ab} \mu_m \mu_n G^* f\left(f + 2f_0\right) + \frac{ab}{4} \left(N_{x0} \lambda_m^2 + N_{y0} \delta_n^2\right)\left(f + f_0\right) \\ &+ \frac{1}{64} \frac{m^2 n^2 \pi^4}{ab} L^* f\left(f + f_0\right)\left(f + 2f_0\right) = q_0 \frac{ab}{mn\pi^2} \mu_m \mu_n \end{aligned} \tag{19}$$

with

$$P^* = P_{11}^* \lambda_m^4 + P_{22}^* \delta_n^4 + (P_{66}^* - 2P_{12}^*) \lambda_m^2 \delta_n^2$$

$$J^* = J_{21}^* \lambda_m^4 + J_{12}^* \delta_n^4 + (J_{11}^* + J_{22}^* - 2J_{66}^*) \lambda_m^2 \delta_n^2$$

$$H^* = H_{11}^* \lambda_m^4 + H_{22}^* \delta_n^4 + (H_{12}^* + H_{21}^* + 4H_{66}^*) \lambda_m^2 \delta_n^2$$

$$G^* = \frac{J_{21}^*}{P_{11}^*} + \frac{J_{12}^*}{P_{22}^*}, L^* = \frac{\delta_n^2}{\lambda_m^2 P_{11}^*} + \frac{\lambda_m^2}{\delta_n^2 P_{22}^*}, \mu_m = 1 - (-1)^m, \mu_n = 1 - (-1)^n, m, n = 1, 2, ...$$

A clamped ES-FGM plate with an immovable edge under simultaneous action of uniformly distributed pressure of intensity q_0 and thermal loads (in a uniform temperature rise environment or

the temperature gradient through the thickness) is considered. The in-plane condition on immovability at all edges, i.e. $u=0$ at $x=0,a$ and $v=0$ at $y=0,b$, is fulfilled in an average sense as [26]:

$$\int_0^b\int_0^a \frac{\partial u}{\partial x}dxdy=0,\ \int_0^a\int_0^b \frac{\partial v}{\partial y}dydx=0 \tag{20}$$

From Eqs. (3), (11) and (12) including the imperfect shape of the plate, we can obtain the relations below:

$$\begin{aligned}
\frac{\partial u}{\partial x}&=P_{22}^*\frac{\partial^2\varphi}{\partial y^2}-P_{12}^*\frac{\partial^2\varphi}{\partial x^2}+J_{11}^*\frac{\partial^2 \mathrm{w}}{\partial x^2}+J_{12}^*\frac{\partial^2 \mathrm{w}}{\partial y^2}-(P_{22}^*-P_{12}^*)\Phi_1-\frac{1}{2}\left(\frac{\partial \mathrm{w}}{\partial x}\right)^2-\frac{\partial w}{\partial x}\frac{\partial w^*}{\partial x}\\
\frac{\partial v}{\partial y}&=P_{11}^*\frac{\partial^2\varphi}{\partial x^2}-P_{12}^*\frac{\partial^2\varphi}{\partial y^2}+J_{22}^*\frac{\partial^2 \mathrm{w}}{\partial y^2}+J_{21}^*\frac{\partial^2 \mathrm{w}}{\partial x^2}-(P_{11}^*-P_{12}^*)\Phi_1-\frac{1}{2}\left(\frac{\partial \mathrm{w}}{\partial y}\right)^2-\frac{\partial w}{\partial y}\frac{\partial w^*}{\partial y}
\end{aligned} \tag{21}$$

Substituting Eqs. (18) into Eqs. (21), and substituting the expression obtained into Eqs. (20) leads to:

$$\begin{aligned}
N_{x0}&=\Phi_1+\frac{1}{8C^*}\left(P_{11}^*\lambda_m^2+P_{12}^*\delta_n^2\right)f\left(f+2f_0\right)\\
&+\frac{n}{mb^2}\mu_m\mu_n\frac{1}{C^*}\left[J_{12}^*P_{11}^*+J_{22}^*P_{12}^*-C^*\frac{J^*}{P^*}\right]f+\frac{m}{na^2}\mu_m\mu_n\frac{J_{11}^*P_{11}^*+J_{21}^*P_{12}^*}{C^*}f\\
N_{y0}&=\Phi_1+\frac{1}{8C^*}\left(P_{12}^*\lambda_m^2+P_{22}^*\delta_n^2\right)f\left(f+2f_0\right)\\
&+\frac{m}{na^2}\mu_m\mu_n\frac{1}{C^*}\left[J_{21}^*P_{22}^*+J_{11}^*P_{12}^*-C^*\frac{J^*}{P^*}\right]f+\frac{n}{mb^2}\mu_m\mu_n\frac{J_{12}^*P_{12}^*+J_{22}^*P_{22}^*}{C^*}f
\end{aligned} \tag{22}$$

where: $C^*=P_{11}^*P_{22}^*-P_{12}^{*2}$

5. Vibration analysis

Suppose that an ES-FGM plate is acted on by a uniformly distributed excited transverse load $q_0=Q_0\sin(\Omega t)$. Substituting Eq. (22) into Eq. (19) to have:

$$\begin{aligned}
&M\ddot{f}(t)+M_1f(t)+M_2(f(t)+f_0)+M_3f(t)(f(t)+f_0)+M_4f(t)(f(t)+2f_0)\\
&+M_5f(t)(f(t)+f_0)(f(t)+2f_0)=M_6
\end{aligned} \tag{23}$$

where:

$$M=\frac{ab}{4}\rho_1;$$

$$M_1=\frac{ab}{4}\left(\frac{J^{*2}}{P^*}+H^*\right);$$

$$M_2=\left(\Phi_1\lambda_m^2\frac{ab}{4}+\Phi_1\delta_n^2\frac{ab}{4}\right);$$

$$M_3 = \frac{2mn\pi^2\mu_m\mu_n}{ab}\frac{J^*}{P^*} + \frac{\lambda_m^2 an}{mb}\frac{1}{C^*}\left[J_{12}^*P_{11}^* + J_{22}^*P_{12}^* - C^*\frac{J^*}{P^*}\right] + \frac{\lambda_m^2 bm}{an}\frac{J_{11}^*P_{11}^* + J_{21}^*P_{12}^*}{C^*} + \frac{\delta_n^2 bm}{anC^*}[\mathrm{J}_{21}^*P_{22}^*$$

$$+\mathrm{J}_{11}^*P_{12}^* - C^*\frac{J^*}{P^*}] + \frac{\delta_n^2 an}{mb}\frac{J_{12}^*P_{12}^* + J_{22}^*P_{22}^*}{C^*}$$

$$M_4 = \frac{1}{6}\frac{mn\pi^2\mu_m\mu_n}{ab}G^*$$

$$M_5 = \frac{1}{64}\frac{m^2n^2\pi^4}{ab}L^* + \frac{\lambda_m^2 ab(P_{11}^*\lambda_m^2 + P_{12}^*\delta_n^2)}{32C^*} + \frac{\delta_n^2 ab}{32}\frac{P_{12}^*\lambda_m^2 + P_{22}^*\delta_n^2}{C^*}$$

$$M_6 = q_0\frac{ab}{mn\pi^2}\mu_m\mu_n$$

Denote: $M_i^* = \frac{M_i}{M}$

Dividing both sides of Equation (23) by M, we have:

$$\begin{aligned}&\ddot{f}(t) + M_1^* f(t) + M_2^*(f(t)+f_0) + M_3^* f(t)(f(t)+f_0) + M_4^* f(t)(f(t)+2f_0)\\&+M_5^* f(t)(f(t)+f_0)(f(t)+2f_0) = M_6^*\end{aligned} \tag{24}$$

in which $M_i^* = \frac{M_i}{M}, (i = 1,2,3,4,5,6)$

Eq. (24) is the governing equation with temperature-dependent coefficients to investigate the nonlinear dynamic response of the eccentrically stiffened FGM plate in thermal environments. The nonlinear dynamic response can be obtained by solving Eq. (24) if the initial conditions are assumed as $f(0) = 0, \dot{f}(0) = 0$ and using the Runge-Kutta method. In the free and linear vibration case, Eq. (24) becomes:

$$\ddot{f}(t) + (M_1^* + M_2^*)f(t) = 0 \tag{25}$$

and the fundamental frequencies of natural vibration of the ES-FGM can be determined by:

$$\omega_L = \sqrt{M_1^* + M_2^*}$$

The equation of nonlinear free vibration of a perfect plate has the form:

$$\ddot{f}(t) + (M_1^* + M_2^*)f(t) + (M_3^* + M_4^*)f^2(t) + M_5^* f^3(t) = 0 \tag{26}$$

To determine the nonlinear vibration frequency of the ES-FGM plate, represent $f(t) = \psi c\cos(\omega t)$ and use a procedure like the Galerkin method for Eq. (26) to obtain:

$$\omega_{NL} = \omega_L\left(1 + \frac{3M_5^*}{4\omega_L^2}\psi^2 + \frac{8(M_3^* + M_4^*)}{3\pi\omega_L^2}\psi\right)^{\frac{1}{2}} \tag{27}$$

In which ω_{NL} is the nonlinear vibration frequency and ψ is the amplitude of nonlinear vibration.

5.1. Uniform temperature rise

In this case, the temperature of the plate is assumed to be uniform, raised from the initial temperature T_i (at which the plate is thermal stress free), to the final temperature T_f and the temperature change $\Delta T = T_f - T_i$. Ignoring the heat transfer through the thickness of the ES-FGM plate, from Eq. (8b) we get:

$$\Phi_1 = -\frac{Ph\Delta T}{1-\nu} \tag{28}$$

where: $\Delta T = const$ and $P = E_m\alpha_m + \frac{E_m\alpha_{cm} + E_{cm}\alpha_m}{k+1} + \frac{E_{cm}\alpha_{cm}}{2k+1}$.

5.2. Through the thickness temperature gradient

In the case where the temperature gradient of the ES-FGM plate is changed through the thickness of the plate, the temperature at the ceramic-rich surface is very high compared to the temperature at the metal-rich surface. By using the one-dimensional Fourier equation, the heat transfer equation through the thickness of the plate can be obtained as:

$$\frac{d}{dz}\left[K(z)\frac{dT}{dz}\right] = 0,\ T(z = h/2) = T_c, T(z = -h/2) = T_m \tag{29}$$

In which T_m, T_c are the temperature at the metal-rich surface and ceramic-rich surface, respectively. The solutions of Eq. (29) can be found in terms of polynomial series, and the first seven terms of this series gives the following approximation:

$$T(z) = T_m + \Delta T\frac{\kappa\sum_{p=0}^{5}\frac{\left(-\kappa^k K_{cm}/K_m\right)^p}{pk+1}}{\sum_{p=0}^{5}\frac{\left(-K_{cm}/K_m\right)^p}{pk+1}} \tag{30}$$

where: $\kappa = \frac{2z+h}{2h}, \Delta T = T_c - T_m$

Substituting Eq. (30) into Eq. (8b) gives:

$$\Phi_1 = -\frac{Lh\Delta T}{1-\nu} \tag{31}$$

where: $L = \frac{\sum_{p=0}^{5}\frac{\left(-K_{cm}/K_m\right)^p}{pk+1}\left[\frac{E_m\alpha_m}{pk+2} + \frac{E_m\alpha_{cm} + E_{cm}\alpha_m}{(p+1)k+2} + \frac{E_{cm}\alpha_{cm}}{(p+2)k+2}\right]}{\sum_{p=0}^{5}\frac{\left(-K_{cm}/K_m\right)^p}{pk+1}}$

6. Numerical results and discussions

In this section, we consider the nonlinear dynamic response of the ES-FGM plates to illustrate the effects of temperature gradient on the properties and vibration response of the ES-FGM plate. Information on the properties of the FGM is given in Table 1, and a Poisson's ratio of 0.3 is chosen for simplicity. The temperature change between the two surfaces is assumed to be constant for simplicity in numerical calculation ($\Delta T = T_c - T_m$).

Table 1. Material properties of the constituent materials of the considered FGM plate [27]

Material	Property	P_0	P_{-1}	P_1	P_2	P_3
Si_3N_4 (Ceramic)	E(Pa)	348.43e9	0	-3.70e-4	2.160e-7	-8.946e-11
	ρ (kg/m^3)	2370	0	0	0	0
	$\alpha(K^{-1})$	5.8723e-6	0	9.095e-4	0	0
	$k(\mathrm{W}/mK)$	13.723	0	0	0	0
SUS304 (Metal)	E(Pa)	201.04e9	0	3.079e-4	-6.534e-7	0
	ρ (kg/m^3)	8166	0	0	0	0
	$\alpha(K^{-1})$	12.330e-6	0	8.086e-4	0	0
	$k(\mathrm{W}/mK)$	15.379	0	0	0	0

Table 2. The fundamental frequencies of natural vibration ω_L (rad/s) of the ES-FGM plates

		ω_L	
(m,n)	k	T-D	T-ID
(1,1)	1	916.4	886.1
	5	835.3	806.5
	10	819.7	791.2
(1,2)	1	1345.7	1290.8
	5	1235.4	1184.2
	10	1213.8	1163.2
(2,2)	1	1641.0	1566.9
	5	1513.1	1444.7
	10	1488.0	1420.4
(1,3)	1	1584.5	1480.3
	5	1487.0	1393.4
	10	1466.0	1374.0
(2,3)	1	1803.2	1683.6
	5	1695.0	1587.9
	10	1672.1	1567.0

The information in Table 2 is calculated with the following geometric parameters:
$h = 0.008$ (m), $s_1 = 0.15$ (m), $s_2 = 0.15$ (m), $h_1 = 0.015$(m), $h_2 = 0.015$ (m), $\mathrm{b}_1 = 0.015$ (m),
$\mathrm{b}_2 = 0.015$ (m), $a = 1.5$ (m), $\mathrm{b} = 1.5$ (m).

Table 2 shows the influence of the numbers (m,n) and volume fraction k on the fundamental frequency of vibration in the two cases of T-D and T-ID. It shows that the increasing numbers (m,n) leads to an increase in the frequency of free vibration. Inversely, the larger the volume fraction k is, the smaller the vibration frequencies are. The ES-FGM plates with T-D have free vibration frequencies larger than ones with T-ID.

Table 3 presents the calculations of fundamental frequencies parameter $\bar{\omega} = \omega_L h\sqrt{\frac{\rho_c}{E_c}}$ for aluminum and alumina in the case of T-D and uniform temperature rise. The result in this case is compared with Matsunaga [3], Bich et al. [15], Alijani et al. [5] and Chorfi and Houmat [6] when $R, R_x, R_y \to \infty$ (FGM plates). Table 3 shows that the results in this paper have great agreement with the results of these abovementioned authors.

Table 3. Comparison of fundamental frequency parameters with the results reported by Matsunaga [3], Bich et al. [15], Alijani et al. [5], and Chorfi and Houmat [6]

k	Present	Matsunaga [3]	Bich et al. [15]	Alijani et al. [5]	Chorfi and Houmat [6]
0	0.0536	0.0588	0.0597	0.0597	0.0577
0.5	0.0384	0.0492	0.0506	0.0506	0.0490
1	0.0340	0.0430	0.0456	0.0456	0.0442
4	0.0286	0.0381	0.0396	0.0396	0.0383
10	0.0268	0.0364	0.0381	0.0380	0.0366

Figs. 2–5 illustrate the effects of geometric parameter fraction b/h on the nonlinear dynamic response of the ES-FGM plate in four cases:

$$case\,1: T-ID, \Delta T = const; \quad case\,2: T-ID, \Delta T = \Delta T(z),$$
$$case\,3: T-D, \Delta T = const; \quad case\,4: T-D, \Delta T = \Delta T(z), \text{ and}$$
$$T_c = 400(K), T_m = 300(K), T_0 = 300(K), \Delta T = const = 100(K), k = 1$$

The effects of the b/h ratio on the nonlinear dynamic response of ES-FGM plates in the four temperature cases were considered. As we can see, when increasing the ratio of b/h, the vibration amplitude increases. These figures show us that the effect of uniform temperature rise is stronger than that of the temperature gradient through the thickness. So, the plate in the case of $\Delta T = \Delta T(z)$ will vibrate with smaller amplitude in both the T-ID and T-D cases. Therefore, the plate will take thermal load better than the case through the thickness temperature gradient (in both T-D and T-ID cases).

Figs. 6–9 consider the influence of temperature on the nonlinear dynamic response for $T_m = 300(K)$, $T_0 = 300(K)$, $k = 1$, $Q = 5000(N/m^2)$, $\Omega = 1000(rad/s)$ with $(T-ID, \Delta T = const)$, $(T-ID, \Delta T = \Delta T(z))$, $(T-D, \Delta T = const)$, $(T-D, \Delta T = \Delta T(z))$, respectively.

It is easy to see that whenever the temperature increases, the amplitude of vibration also increases. Similar to the case of uniform temperature rise, the vibration of the ES-FGM is larger than the temperature change through the thickness case. Furthermore, if we compare the T-D case with the T-ID case, we show that if properties of the plate are temperature-dependent, the plate will vibrate more strongly than the case where the properties are temperature-independent.

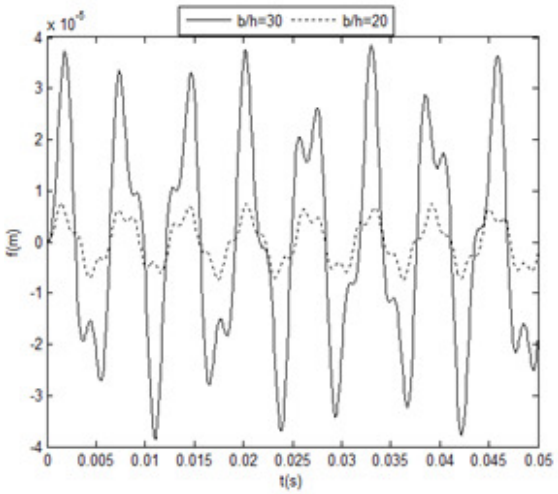

Fig. 2. Effect of b/h on nonlinear dynamic response of ES-FGM plate in case (T-ID, $\Delta T = const$)

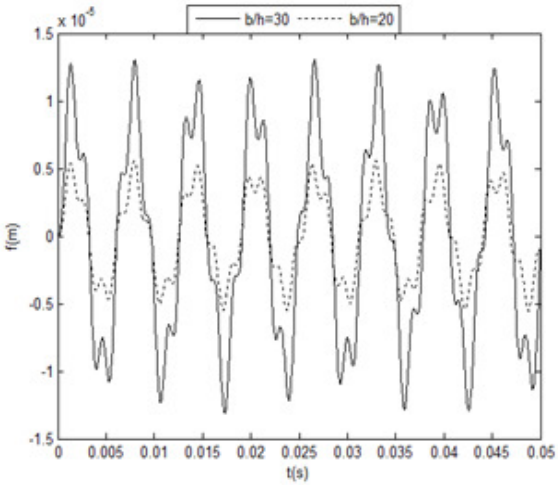

Fig. 3. Effect of b/h on nonlinear dynamic response of ES-FGM plate in case (T-ID, $\Delta T = \Delta T(z)$)

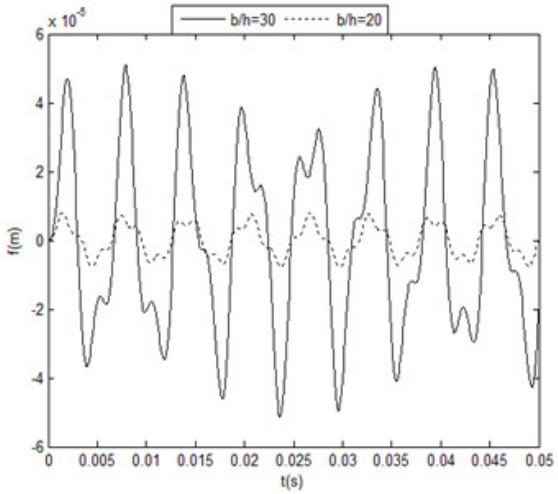

Fig. 4. Effect of b/h on nonlinear dynamic response of ES-FGM plate (T-D, $\Delta T = const$)

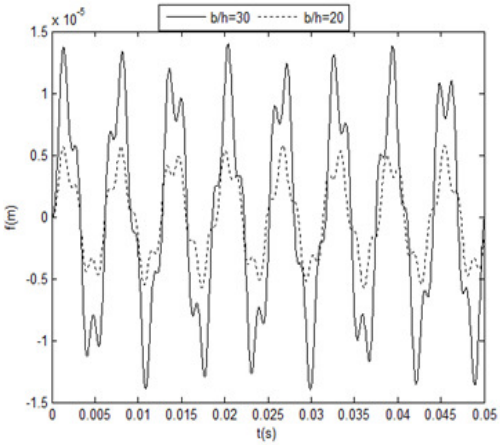

Fig. 5. Effect of b/h on nonlinear dynamic of ES-FGM plate (T-D, $\Delta T = \Delta T(z)$)

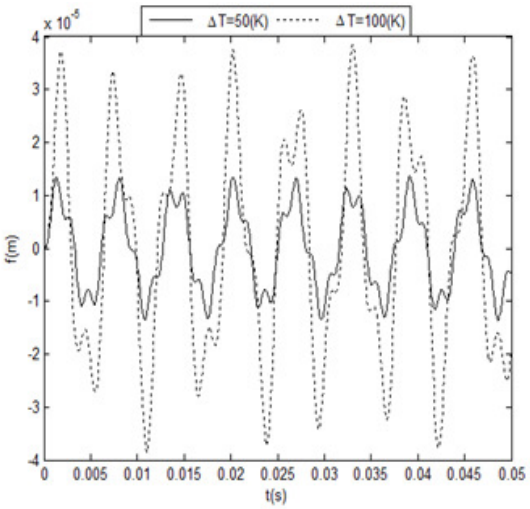

Fig. 6. Influence of uniform temperature rise on nonlinear response of the plate $(T-ID, \Delta T = const)$

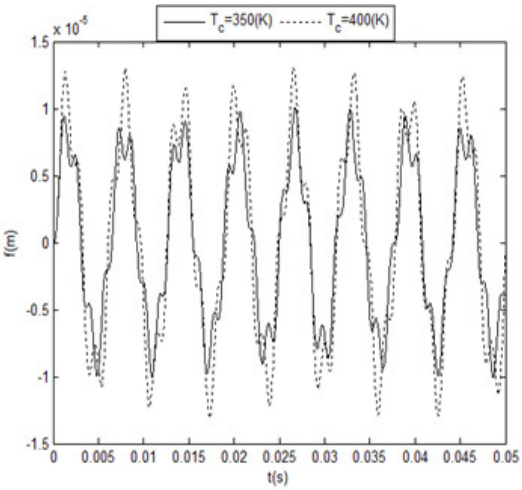

Fig. 7. Influence of through the thickness temperature gradient on nonlinear response of the plate $(T-ID, \Delta T = \Delta T(z))$

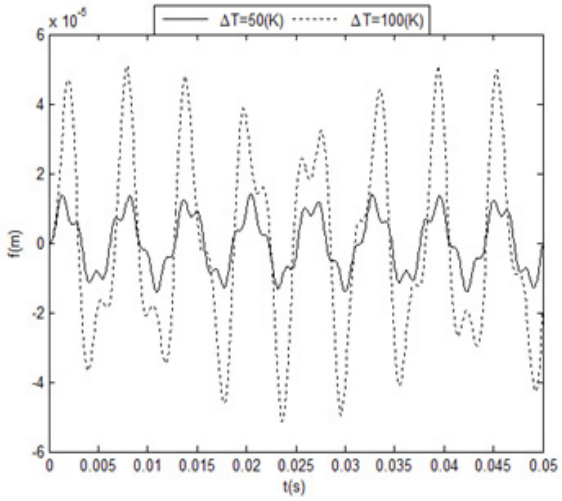

Fig. 8. Temperature-dependent nonlinear dynamic response with $T-D, \Delta T = const$.

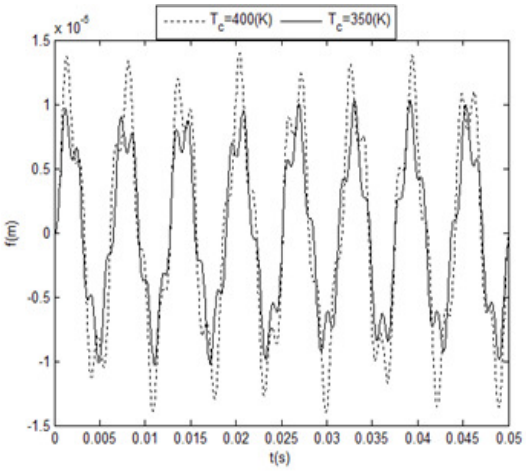

Fig. 9. Temperature-dependent nonlinear dynamic response with $T-D, \Delta T = \Delta T(z)$

Figs. 10–13 describe the nonlinear vibration of the ES FGM plates depending on initial imperfection of the plates. Obviously, the amplitude of vibration will increase and lose stability if the initial imperfection increases. These figures below are considered in four cases:

$(T-ID, \Delta T = const), (T-ID, \Delta T = \Delta T(z)), (T-D, \Delta T = const), (T-D, \Delta T = \Delta T(z))$

with parameters of the plate of:

$k=1, T_c=400(K), T_m=300(K), T_0=300(K), \Delta T=100(K),$
$Q_0=5000(N/m^2), \Omega=1000(rad/s)$

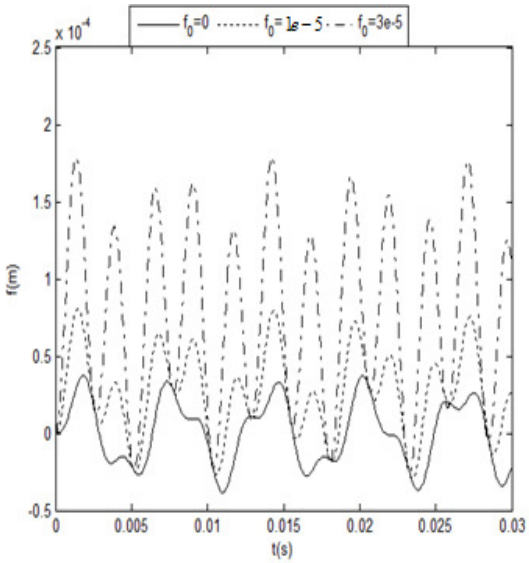

Fig. 10. Impact of initial imperfection on nonlinear response of the plate $(T-ID, \Delta T=const)$

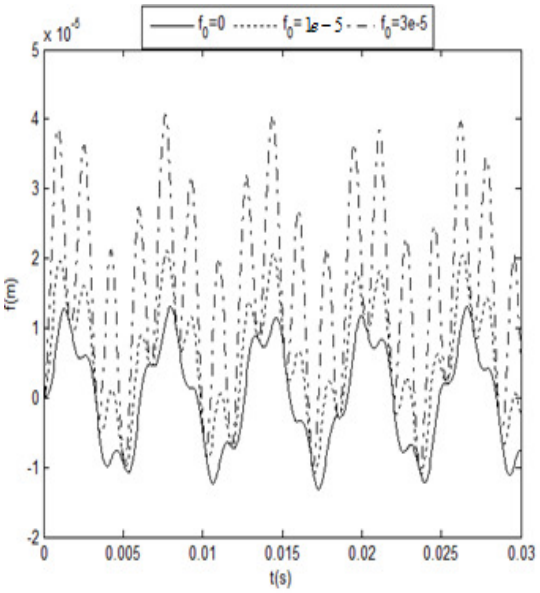

Fig. 11. Impact of initial imperfection on nonlinear response of the plate $(T-ID, \Delta T=\Delta T(z))$

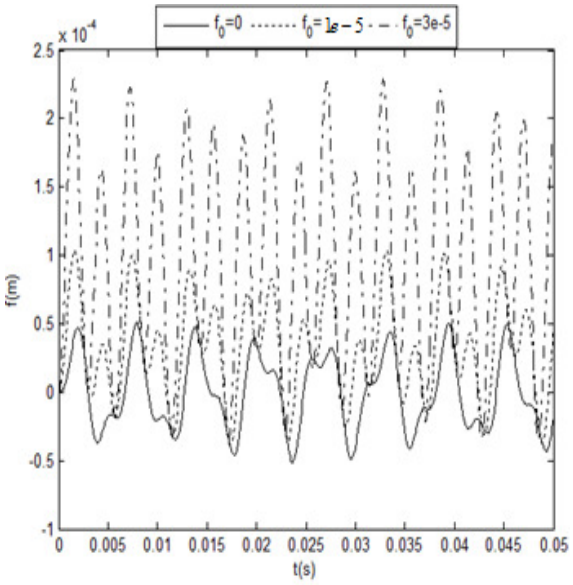

Fig. 12. Impact of initial imperfection on nonlinear response of the plate $(T-D, \Delta T=const)$

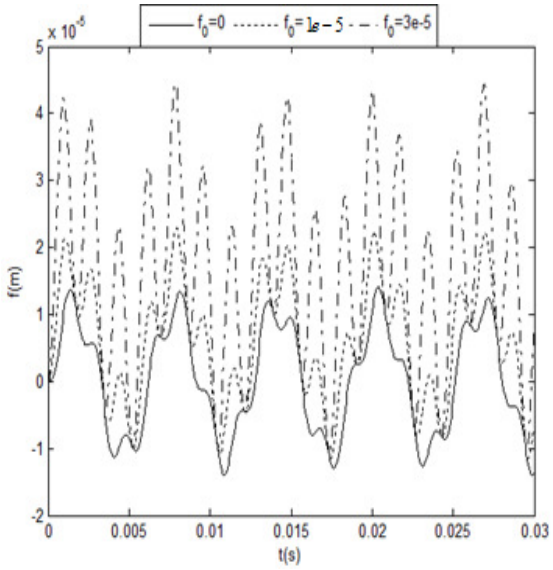

Fig. 13. Impact of initial imperfection on nonlinear response of the plate $(T-D, \Delta T=\Delta T(z))$

Figs. 14 and 15 show us the influence of volume fraction on the nonlinear dynamic response of the ES-FGM plate. As the volume fraction increases, the nonlinear response amplitude increases as a result. This is explained by the fact that the increase of volume fraction k makes the ceramic component decrease, while the Young's modulus of ceramic is greater than that for metal. Computations have been carried out for the following material and parameters of the plate:

$$k=1, T_c=400(K), T_m=300(K), T_0=300(K), \Delta T=100(K), Q_0=5000(N/m^2); \Omega=1000(rad/s)$$

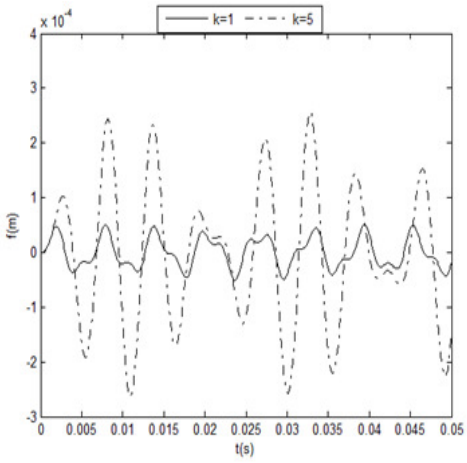

Fig. 14. Volume fraction-nonlinear vibration amplitude relation with $T-D, \Delta T=const$

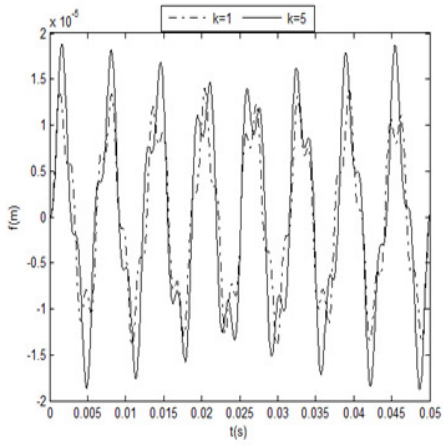

Fig. 15. Volume fraction-nonlinear amplitude relation with $T-D, \Delta T=\Delta T(z)$

In Fig. 16 and Fig. 17, the relationship of frequency-amplitude of nonlinear free vibration of the plate (obtained from Eq. (27)) will be represented with $(m,n)=(1,1), \Delta T=50(K), \Delta T=100(K), k=1, k=5$ in the uniform temperature rise case and $(m,n)=(1,1), T_m=300(K),\ T_c=350(K), T_c=450(K), k=1, k=5$ in the through the thickness temperature rise case.

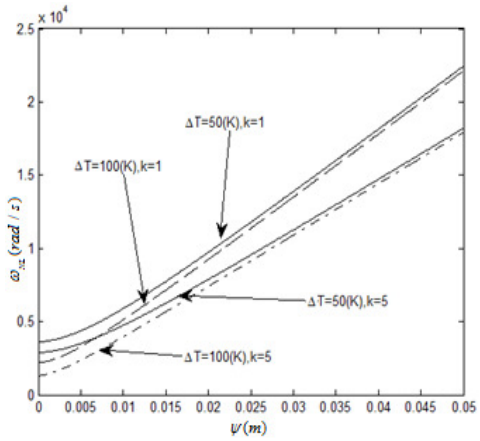

Fig. 16. Frequency-amplitude relation with $T-D, \Delta T=const$

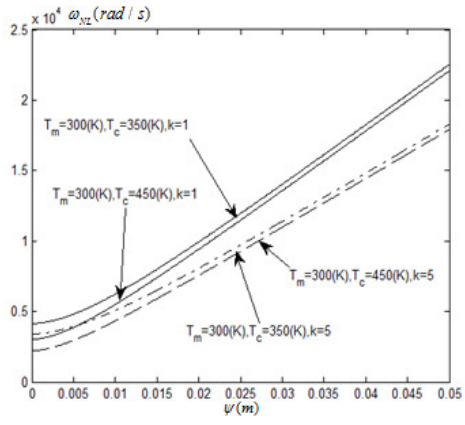

Fig. 17. Frequency-amplitude relation with $T-D, \Delta T=\Delta T(z)$

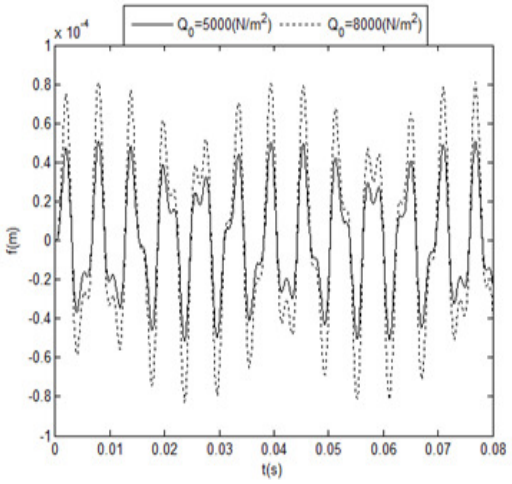

Fig. 18. Effect of amplitude Q_0 on nonlinear response with $T-D, \Delta T = const$

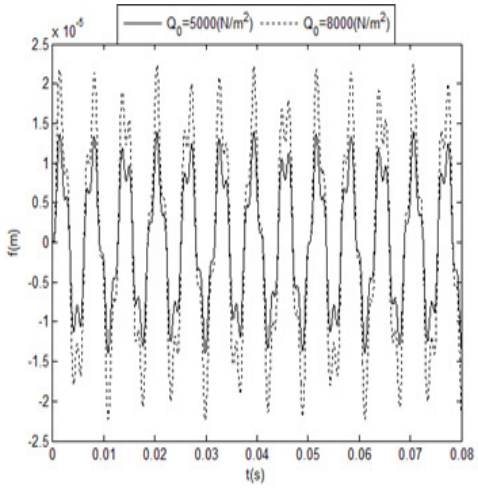

Fig. 19. Effect of amplitude Q_0 on nonlinear response with $T-D, \Delta T = \Delta T(z)$

The effect of amplitude Q_0 of uniformly distribution load q_0 on the nonlinear response of the ES-FGM plate is illustrated in Figs. 18 and 19. The calculations in Figs. 18 and 19 are performed with parameters:

$k = 1, T_0 = 300(K), T_c = 400(K), T_m = 300(K), \Delta T = 100(K), \ \Omega = 1000(rad/s)$

7. Concluding remarks

The vibration and nonlinear dynamic response of the thin ES-FGM plate in thermal environments are investigated in this paper. From the obtained results, we can conclude that:

- the stiffeners strongly enhance the mechanical and thermal load-carrying capacity of the FGM plate

- the mechanical and thermal load-carrying capacity of the FGM plate in the T-ID case is better than the plate in the T-D case

- the effect of uniform temperature rise is stronger than the effect of through the thickness temperature gradient. So, the plate in the case of $\Delta T = \Delta T(z)$ will vibrate with smaller amplitude in both T-ID and T-D cases

- the initial imperfection, volume fraction index, geometrical parameters and temperature have a strong effect on the nonlinear dynamic response and nonlinear vibration of the ES-FGM plates.

Acknowledgement

This work was supported by the Grant of Newton Fund (UK), code: NRCP1516/1/68. The authors are grateful for this support.

References

[1] Woo J, Meguid SA, Ong LS. Journal of Sound and Vibration. 2006, 289, 595-611.

[2] Wu TL, Shukla KK, Huang JH. International Journal of Applied Mechanics and Engineering. 2006, 11, 679-98.

[3] Matsunaga H. J. Composite Structures. 2008, 82, 499-512.

[4] Allahverdizadeh A, Naeiand MN, Nikkhah Bahrami M. Journal of Sound and Vibration. 2008, 310, 966-84.

[5] Alijani F, Amabili M, Karagiozis K, Bakhtiari-Nejad F. Journal of Sound and Vibration. 2011, 30, 1432-54.

[6] Chorfi SM, Houmat A. J. Composite Structures. 2010, 92, 2573-81.

[7] Kim KD, Lomboy GR, Han SC. Journal of Composite Materials. 2008, 42, 485-511.

[8] Mollarazi HR, Foroutan M, Moradi-Dastjerdi R. Journal of Composite Materials. 2011, 46, 507-515.

[9] Reza Jahanghiry, Rajab Yahyazadeh, Naser Sharafkhani, Vahid A. Maleki. Science and Engineering of Composite Materials, doi: 10.1515/secm-2014-0079, 2014.

[10] Kamran Asemi, Manouchehr Salehi, Mehdi Akhlaghi. Science and Engineering of Composite Materials. doi: 10.1515/secm-2013-0346, 2014.

[11] Huang X, Shen HS. International Journal of Solid and Structures. 2014, 41, 2403-427.

[12] Kim YW. Journal of Sound and Vibration. 2005, 284, 531-49.

[13] Fakhari V, Ohadi A. Journal of Vibration and Control. 2010 DOI: 10.1177/1077546309354970.

[14] Bich DH, Nam VH, Phuong NT. Vietnam Journal of Mechanics. 2011, 33, 131-47.

[15] Bich DH, Dung DV, Nam VH. J. Composite Structures. 2012, 94, 2465-73.

[16] Duc ND. J. Composite Structures. 2013, 102, 306-14.

[17] Duc ND, Quan TQ. J. Composite Structures. 2013, 106, 590-600.

[18] Duc ND, Cong PH. J. Thin-Walled Structures. 2014, 75, 103-12.

[19] Bich DH, Duc ND, Quan TQ. International Journal of Mechanical Sciences. 2014, 80, 16-28.

[20] Quan TQ, Phuong Tran, Tuan ND, Duc ND. J. Composite structures. 2015, 126, 16-33.

[21] Duc ND, Cong PH. Journal of Vibration and Control. 2015, 21, 637-646.

[22] Duc ND, Quan TQ. Journal of Vibration and Control. 2015, 21, 1340-1362.

[23] Cong PH, An PTN, Duc ND. Science and Engineering of Composite Materials. Accepted for publication 2015.

[24] Duc ND. Nonlinear Static and Dynamic Stability of Functionally Graded Plates and Shells. Vietnam National University Press, Hanoi, 2014.

[25] Volmir AS. Nonlinear dynamics of plates and shells. Science Edition. Moscow, 1972.

[26] Duc ND, Tung HV. J. Mechanics of Composite Materials. 2010, 46, 461-76.

[27] Reddy JN, Chin CD. Journal of thermal Stresses. 1998, 21, 593-626.